International Journal of Nanomedicine

Dovepress
Taylor & Francis Group

Open Access Full Text Article

ORIGINAL RESEARCH

Aptamer Functionalized Liposomes Co-Loaded with Exenatide-4 and Coenzyme Q10 Ameliorate Type 2 Diabetes Mellitus by Improving Pancreatic β Cell Function

Shangying Xiao[1], Lei Rao[2], Canying Yan[1], Ling Nie[1], Leiqi Wang[1], Yingyin Zhao[1], Shihao Zhang[1], WeiMao Zhan[1], Dongyun Qin[1], Manjiao Zhuang[1]

[1]Guangdong Provincial Key Laboratory of Research and Development of Natural Drugs, and School of Pharmacy, Guangdong Medical University, Dongguan, People's Republic of China; [2]Medical College, Shaoguan University, Shaoguan, People's Republic of China

Correspondence: Dongyun Qin; Manjiao Zhuang, Guangdong Provincial Key Laboratory of Research and Development of Natural Drugs, and School of Pharmacy, Guangdong Medical University, Dongguan, People's Republic of China, Tel +15692005207, Email 410136762@qq.com; man.jiao@163.com

Introduction: Oxidative stress has been shown to disrupt β-cell function and promote the development of type 2 diabetes mellitus (T2DM). Exenatide-4 (Ext-4) is a widely used anti-glycemic drug but cannot restore pancreatic β-cells' structure and function. Coenzyme Q10 (CoQ10) has great antioxidant activities but shows suboptimal therapeutic effects because of its poor solubility and poor bioavailability. To further enhance the therapeutic efficacy of the drugs, a pancreas-targeting liposomal co-delivery system encapsulating Ext-4 and CoQ10 ((E+Q)-Lip-Apt) was designed, using the aptamers as the targeting ligands.

Methods: (E+Q)-Lip-Apt was prepared by thin film dispersion method and its optimal formulation was obtained through single-factor experiments and orthogonal experiments. The pancreatic β-cell protecting effect of (E+Q)-Lip-Apt was investigated both in vitro and in vivo.

Results: (E+Q)-Lip-Apt exhibited uniform size, good dispersion, and high encapsulation efficiency (EE) for both Ext-4 and CoQ10. The in vitro results showed that (E+Q)-Lip-Apt manifested superior capacity in scavenging ROS, enhancing mitochondrial membrane potential, and reducing malondialdehyde (MDA) content compared to Ext-4 in MIN6 cells. In vivo investigations demonstrated that (E+Q)-Lip-Apt significantly improved glucose tolerance, insulin sensitivity, hepatic lipid metabolism, oxidative stress, and enhanced antioxidant enzyme activity in diabetic mice. Moreover, Hematoxylin-eosin staining (H&E) and Immunohistochemistry (IHC) results indicated that (E+Q)-Lip-Apt could improve liver and pancreatic lesions, restoring the structure and function of β-cells in diabetic mice.

Conclusion: (E+Q)-Lip-Apt could improve oxidative stress, thereby restoring pancreatic β-cell function, and alleviating diabetes.

Keywords: liposomes, type 2 diabetes mellitus, oxidative stress, targeted therapy, reactive oxygen species

Introduction

Diabetes is one of the most common chronic metabolic diseases. According to the International Diabetes Federation (IDF), it is estimated that by 2030, the number of diabetes patients will reach 643 million, and by 2045, the number of people with diabetes worldwide could reach 783 million.[1] Type 2 diabetes mellitus (T2DM) patients account for 90% of diabetes patients.[2,3] The annual cost of diabetes treatment globally is high; nevertheless, millions of diabetes patients still die each year.[1] Therefore, the efficient treatment of T2DM is extremely important for widespread patients.

The preservation and restoration of functional β-cells are crucial to the treatment of T2DM.[4] Clinical diagnoses have demonstrated that most T2DM patients have a 70%~90% reduction in β-cells.[5] Mitochondrial reactive oxygen species (ROS) are the main source of endogenous ROS, produced in the mitochondrial electron transport chain. Continuous high-glucose conditions can lead to increased oxygen consumption by mitochondria and mitochondrial dysfunction, oxidative stress imbalance, excessive accumulation of ROS, progressive dysfunction of pancreatic β-cells, insulin resistance, and the

Received: 4 December 2024
Accepted: 11 February 2025
Published: 17 March 2025

Graphical Abstract

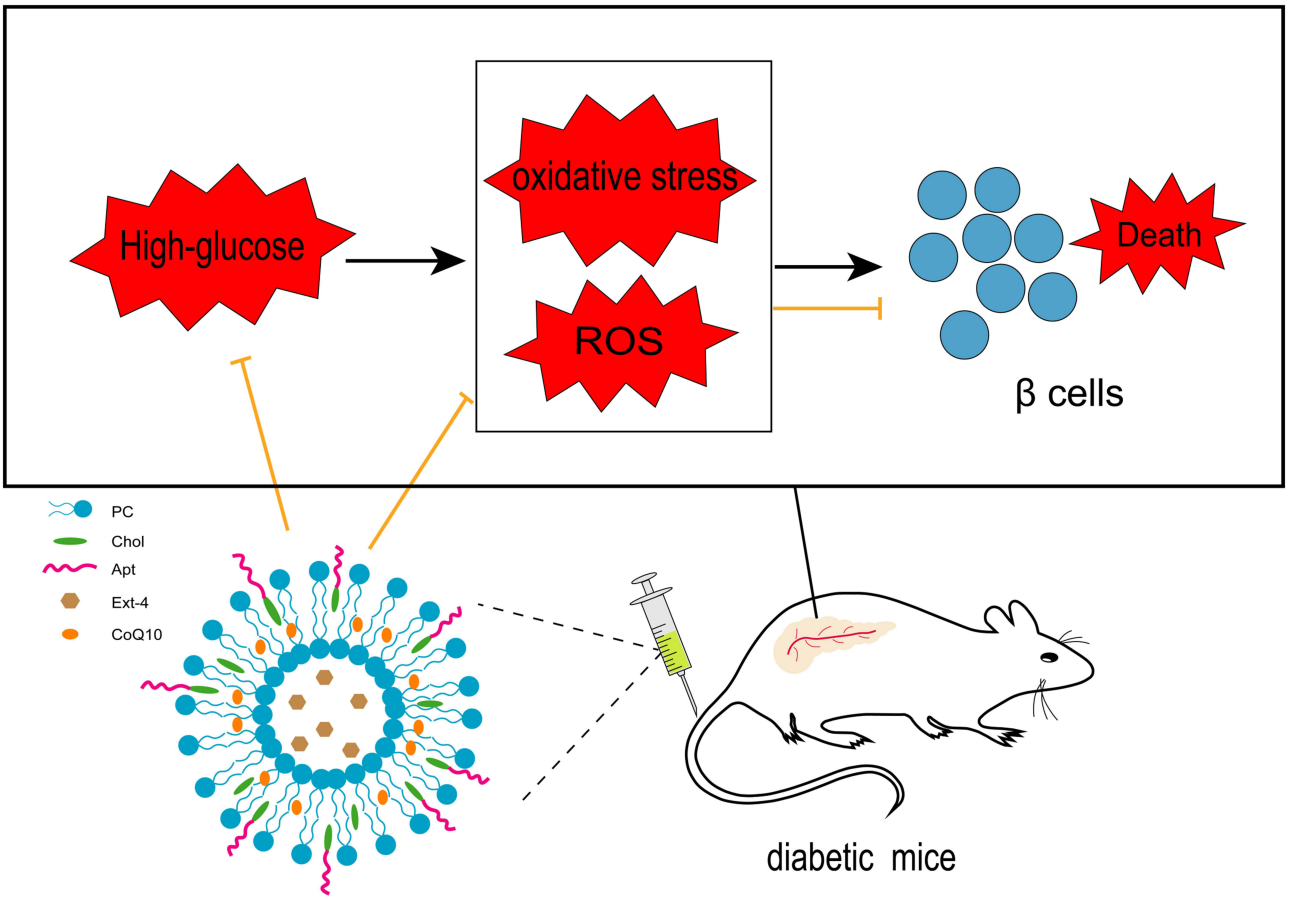

occurrence of various diabetes complications.[3] Therefore, in addition to promoting insulin secretion, preventing pancreatic β-cell apoptosis via reducing ROS is also an important strategy for treating T2DM.

Due to the continuous development of insulin resistance and functional destruction of pancreatic β-cells, the therapeutic effects of insulin or other antidiabetic drugs such as metformin, dipeptidyl peptidase-4 inhibitors (DPP-4), and GLP-1 receptor agonists (GLP-1 RA) have certain limitations. Long-term use also presents side effects such as hypoglycemia, weight gain, renal function impairment, gastrointestinal discomfort, and so on.[6–8] GLP-1 RA is the first-line injectable therapy for T2DM. Exenatide-4 (Ext-4) is the first GLP-1 RA drug to be marketed, which can effectively reduce cardiovascular diseases and promote insulin secretion. However, like other antidiabetic drugs, it cannot prevent the apoptosis of pancreatic β-cells.[7] Moreover, the short half-life of Ext-4 is not conducive to its clinical application. Coenzyme Q10 (CoQ10) has many important functions within cells, playing a key role in the electron transport chain and electron transfer in mitochondria.[9] Additionally, as an endogenous antioxidant, studies have shown that the mechanism by which CoQ10 enhances insulin sensitivity includes the regulation of insulin and adiponectin receptors, tyrosine kinase (TK), phosphoinositide 3-kinase (PI3K), glucose transport proteins, as well as improving lipid profiles, redox systems, advanced glycation end-products receptors (sRAGE), and adipokines.[10] However, the poor water solubility of CoQ10 limits its application and effectiveness.

Liposomes are orderly arranged single or multilayer vesicles synthesized from phospholipids and cholesterol. The properties of liposomes are mainly determined by phospholipids[11] while cholesterol improves the stability of liposomes.[12] Compared to other nanomaterials, the composition of liposomes is similar to that of cell membranes,

which have high biocompatibility and low toxicity.[13,14] Meanwhile, liposomes have a unique bilayer structure that can encapsulate water-soluble drugs in the center of liposomes and encapsulate fat-soluble molecules in the phospholipid molecular layer. Liposomal drug products have been successfully marketed and applied to different clinical practices.[14,15]

Aptamers (Apt) are a new class of single-stranded oligonucleotides with excellent specificity and affinity for target molecules.[16–18] Compared to protein antibodies, Apt has many advantages, such as high specificity, non-immunogenic, ease of synthesis, and ease of modification.[19–21] In recent years, apt-functionalized nano-drug delivery systems have been widely applied in the research of various diseases.[18,22] Pancreatic polypeptide is a hormone secreted by polypeptide cells located around the islets of Langerhans. Research shows that compared to healthy people, T2DM patients have significantly increased levels of pancreatic polypeptide in their bodies.[23] Research has shown that the Apt with the sequence (5' to 3') CGTGCAATGTCGAATGCATGAGCAAACATGGCGAT binds efficiently to tryptic polypeptides.[24]

In this study, Ext-4 and CoQ10 were loaded simultaneously in liposomes, and the attachment between aptamers and liposomes was achieved by modifying the cholesterol at the 5' end of the aptamer.[19] In this way, the prepared liposomes not only improved the stability and half-life of Ext-4, enhanced the water solubility and bioavailability of CoQ10, but also enabled the liposomes to achieve active targeting delivery to the pancreas under the mediation of aptamers, facilitating the therapeutic effect of the drugs in the pancreas. Ext-4 could better promote insulin secretion, while CoQ10 could more effectively achieve antioxidant effects, restoring the function and amount of pancreatic β-cells, and fundamentally improving diabetes symptoms, thereby providing new treatment directions for T2DM.

Materials and Methods

Materials

CoQ10 and Ext-4 were purchased from Med Chem Express (Guangzhou, China); Phosphatidylcholine (PC), cholesterol (Chol), and streptozotocin (STZ) were purchased from Aladdin Biochemical Technology (Shanghai, China). Aptamer with the sequence (5'-3') Cholesteryl-CGTGCAATGTCGAATGCATGAGCAAACATGGCGAT-FAM (FAM is a fluorescent dye) was purchased from Sangon Biotech (Shanghai, China). Glycated hemoglobin ELISA kit and Mouse insulin ELISA kit were purchased from Jiangsu Enzyme Exemption Industry (Jiangsu, China). JC-1 and DCFH-DA kits were purchased from Beyotime Biotechnology (Shanghai, China), The malondialdehyde (MDA) content test kit, superoxide dismutase (SOD) activity test kit and total cholesterol (TC) test kit were purchased from Solarbio (Beijing, China). The triglyceride (TG) test kit and low-density lipoprotein cholesterol (LDL-C) test kit were purchased from Nanjing Jiancheng Bioengineering Institute (Nanjing, China).

Method

Formulation Study of (E+Q)-Lip-Apt

(E+Q)-Lip-Apt was prepared based on CoQ10-Lip. Therefore, the first step in the formulation study of (E+Q)-Lip-Apt was to investigate the optimal formulation of CoQ10-Lip. The effects of ultrasound time, power, the molar ratio of phosphatidylcholine to cholesterol (PC: Chol), and the mass ratio of CoQ10 to lipids (CoQ10: lipids) on encapsulation efficiency (EE) of CoQ10 were Investigated through the single-factor experiment. Then, the optimal formulation of CoQ10-Lip was obtained through orthogonal design assistant software (II V3.1) and experiments. Finally, based on the optimal formulation of CoQ10-Lip, an appropriate amount of Ext-4 was added to prepare the optimized (E+Q)-Lip-Apt.

Preparation of (E+Q)-Lip-Apt

The optimized formulation of (E+Q)-Lip-Apt consisted of 60.00 mg PC, 15.22 mg Chol, and 7.52 mg CoQ10, dissolved in chloroform. The chloroform was then removed by rotary vacuum evaporation, followed by hydration with a PBS solution of Ext-4. Then, the apt solution was added, and the mixture was sonicated to obtain (E+Q)-Lip-Apt.

Characterization of Liposomes

Size, Polydispersity Index (PDI), and Zeta Potential (ZP)

Liposomes were diluted with water, and the Size, PDI, and ZP were determined using the particle size analyzer (HORIBA, SZ-100, Japan).

Encapsulation Efficiency of CoQ10 (EE_{CoQ10})

The absorbance of the CoQ10 mixture was determined at 275 nm using a UV–vis spectrophotometer (SHIMADZU UV-2600i, Suzhou, China). The free CoQ10 was separated from liposomes by low-speed centrifugation. The upper supernatant of the liposomes was taken and demulsified to calculate the mass of encapsulated CoQ10. An equal amount of uncentrifuged liposome solution was taken and demulsified to calculate the total CoQ10. The EE of CoQ10 using Eq. (1):

$$EE_{CoQ10}(\%) = \frac{\text{The mass of encapsulated CoQ10}}{\text{The mass of total CoQ10}} * 100 \quad (1)$$

Encapsulation Efficiency of Ext-4 ($EE_{Ext\text{-}4}$)

The BCA kit was used to quantify Ext-4. Ext-4 was separated from liposomes by high-speed centrifugation at 4°C in a 50 kDa ultrafiltration tube. The filtrate from the lower tube was collected to measure the free Ext-4 mass. An equal amount of uncentrifuged liposome solution was taken and demulsified to measure the total Ext-4 mass. The EE of Ext-4 using Eq. (2)

$$EE_{Ext-4}(\%) = (1 - \frac{\text{Free Ext} - 4\,\text{mass}}{\text{Total Ext} - 4\,\text{mass}}) * 100 \quad (2)$$

Aptamer Conjugation Efficiency (CE)

The 3' end of the aptamer was modified with FAM. The free aptamers were separated from liposomes by high-speed centrifugation using a 50 kDa ultrafiltration tube. The lower filtrate contained free aptamer, while the upper solution contained Apt-Lip. The fluorescence intensity of the upper solution was measured, which corresponded to the fluorescence intensity of the Apt-liposomes. An equal amount of uncentrifuged liposome solution was taken to measure the total fluorescence intensity. The CE of Apt using Eq: (3)

$$CE_{Apt}(\%) = \frac{\text{Fluorescence intensity of Apt} - \text{Lip}}{\text{Total fluorescence intensity}} * 100 \quad (3)$$

Morphological Characterization

The (E+Q)-Lip-Apt was placed onto a copper grid and stained. After natural drying, the size and morphology of the liposomes were observed under a transmission electron microscope (TEM).

In Vitro Study of (E+Q)-Lip-Apt

Cell Culture

Mouse pancreatic β-cells (MIN6) were obtained from the Bowers Type Culture Collection (BTCC, Beijing, China,). MIN6 cells were cultured in RPMI-1640 with 10% Fetal Bovine Serum (FBS) and 1% penicillin-streptomycin and cultured at 37 °C in a 5% CO_2 incubator.

Biocompatibility Analysis

MIN6 cells were plated overnight in a 96-well plate, after which the medium was exchanged for RPMI-1640 medium containing (E+Q)-Lip-Apt (0.057, 0.285, 0.855, 1.71 μM). After 24 h, cell viability was assessed with a CCK-8 kit.

Cell Viability

MIN6 cells were plated overnight in a 96-well plate, after which the complete medium was removed. Then the control (CON) group was treated with RPMI-1640 medium, while the other groups were treated with 200 μM Tert-Butyl Hydroperoxide (TBHP), or with a mixture of 200 μM TBHP and Ext-4 or (E+Q)-Lip-Apt (equal to Ext-4) for 24 h. Cell viability was assessed using CCK-8 kit.

MDA Content Analysis

MIN6 cells were plated in a 10 cm culture dish and cultured with a cell density of 80%. Next, the complete medium was removed. The CON group was treated with RPMI-1640 medium, while the TBHP group was treated with 200 μM TBHP,

the Ext-4 group was treated with a mixture of 200 μM TBHP and 0.285 μM Ext-4, the (E+Q)-Lip-Apt group was treated with a mixture of 200 μM TBHP and (E+Q)-Lip-Apt (equal to Ext-4). After 24 h, the cells were collected and disrupted to assess the MDA content using the MDA content detection kit.

Intracellular ROS Analysis

Intracellular ROS levels were evaluated using the DCFH-DA probe. MIN6 cells were plated overnight in a 6-well plate, after which the complete medium was removed. Cells were washed with PBS and stained for 20 min with DCFH-DA probe. The excess probe was washed with PBS. Next, the CON group was treated with RPMI-1640 medium, while the other groups were treated with 200 μM TBHP, or with a mixture of 200 μM TBHP and Ext-4 (0.285 μM) or (E+Q)-Lip-Apt (equal to Ext-4) for 6 h. A fluorescence microscope was used to image cells (EVOS FL Auto, Life technologies Bothell, USA).

Measurement of Mitochondrial Membrane Potential

MIN6 cells were plated overnight in a 6-well plate, after which the complete medium was removed. Next, the CON group was treated with RPMI-1640 medium, while the other groups were treated with 200 μM TBHP, or with a mixture of 200 μM TBHP and Ext-4 (0.285 μM) or (E+Q)-Lip-Apt (equal to Ext-4) for 24 h. Next, cells were washed with PBS and stained for 15 min with JC-1 probe. The excess probe was washed with PBS and cells were then imaged via confocal laser scanning microscopy (Leica SP8, Germany).

In Vivo Study of (E+Q)-Lip-Apt

Study Design

The SPF-grade male C57BL/6J mice (6 weeks old, approximately 20 g) were purchased from Zhuhai Bestest Biotechnology (Zhuhai, China) and were housed at the Animal Experiment Center of Guangdong Medical University. All animal experiments were conducted with the approval of the Animal Ethics Committee of Guangdong Medical University [Approval No.: GDY2102488], and procedures were performed in accordance with the Chinese Laboratory animal-guideline for ethical review of animal welfare. Housing conditions were 12 h of light and 12 h of darkness, (25 ± 2) °C, (55 ± 5) % humidity, and mice were free to access food and water.

After one week of adaptive feeding, mice were randomly divided into a normal control group (CON, n=8) and a high-fat diet group (HFD, n=30). After 4 weeks of HFD, the HFD mice were intraperitoneally injected with streptozotocin (STZ, 50 mg/kg, dissolved in 0.1 M sodium citrate buffer) for 5 consecutive days. Seven days after the final injection, fasting blood glucose (FBG) levels of the mice were measured, and mice with FBG ≥ 11.1 mmol/L were used as T2DM mice. Next, the diabetic mice were randomly divided into three groups, with 10 mice in each group: T2DM group (DM), Ext-4 group, and (E+Q)-Lip-Apt group. During the experiment, the mice had free access to water and food. The CON group was fed a normal diet, while the diabetic mice continued on a high-fat diet. The CON group and DM group received daily intravenous injections of saline, the Ext-4 group received daily subcutaneous injections of Ext-4 (240 mg/kg), and the (E+Q)-Lip-Apt group received daily intravenous injections of (E+Q)-Lip-Apt (equal to Ext-4). The treatment lasted 8 weeks but one diabetic mouse in the DM group was sacrificed during the experiment.

Intraperitoneal Insulin Tolerance Test (IPITT)

After 6 weeks of treatment, mice were fasted for 4 h, intraperitoneally injected with insulin (0.75U/kg), and blood glucose levels were measured at 0, 30, and 60 min after insulin injection.

Oral Glucose Tolerance Test (OGTT)

After 7 weeks of treatment, mice were fasted for 12 h and then gavaged with glucose solution (2 g/kg). Blood glucose levels were measured at 0, 30, 60, 90, and 120 min after gavage.

Assessment of TG, TC, LDL-C, MDA Content, and SOD Activity

The ground liver tissue was tested for TG content, total TC content, LDL-C content, and SOD activity. All test procedures and the calculation of results were carried out exactly, according to the instructions.

Ex Vivo Imaging

To demonstrate that the liposomes we prepared had excellent specificity and affinity for islets, the mice were anesthetized and dissected to obtain their liver, heart, pancreas, and kidneys after the experiment, which were imaged by Small Animal In Vivo Imaging (IVIS Lumina III, PerkinElmer). The average fluorescence intensity was analyzed to determine the distribution of (E+Q)-Lip-Apt.

Statistical Analysis

All experiments in this study were repeated at least three times, and all data were presented as mean ± standard deviation (SD). Data processing was performed using GraphPad Prism 9.5, and One-way ANOVA was used for data difference testing, with $P < 0.05$ as the threshold of significance.

Results

Single-Factor Analysis of CoQ10-Lip

The film dispersion method was used to prepare liposomes, the results showed that ultrasonic power, ultrasonic time, the molar ratio of PC to Chol, and the mass ratio of CoQ10 to lipids all had varying degrees of impact on the EE of CoQ10, with EE ranging from (55.37±0.25) % to (88.09±0.10) % (Table S1~S4). Thus, an orthogonal design was necessary to provide the best possible combination of these factors.

Orthogonal Design of CoQ10-Lip

The orthogonal design L_9 (4^3) was used to optimize the formulation (Tables 1 and 2). The results of Intuitive analysis showed that the main factors affecting EE of CoQ10 were D>B>A>C, and the optimal combination was $A_3B_3C_1D_3$, with a ratio of PC: Chol (2:1), a ratio of CoQ10: Lipids (10:1), an ultrasound power of 100 W, and an ultrasound time of 15 minutes (Table 2 and Figure 1). (E+Q)-Lip-Apt was prepared based on $A_3B_3C_1D_3$ by adding Ext-4.

Characterization of (E+Q)-Lip-Apt

The physical characterization of the five distinct liposomes was summarized in Table 3. The particle size increased after the variety of encapsulated drugs increased. The size and ZP of (E+Q)-Lip were (107.4 ± 3.5) nm and (−15.2 ± 3.0) mV, respectively. Moreover, the size and surface charge of the liposomes increased slightly after aptamers modification. The size of (E+Q)-Lip-Apt was (112.4 ± 2.2) nm, and the ZP was (−16.3 ± 1.9) mV. As shown in (Figure 2A), the (E+Q)-Lip-Apt solution was yellow, clarified, and did not appear to be precipitated within 18 days, and after 18 days the size and ZP were (137.3±3.0) nm and (−14.8±1.4) mV, which demonstrated the good stability of (E+Q)-Lip-Apt. Subsequently, (E+Q)-Lip-Apt was further characterized by TEM, and (Figure 2B) demonstrated that it was spherical and homogeneous in morphology. (Figure 2C and D) showed that the size and ZP of (E+Q)-Lip-Apt exhibited a unimodal distribution, with $EE_{Ext\text{-}4}$ was (71.59 ± 15.86) % and EE_{CoQ10} was (98.16 ± 0.20) % (Table 3). These results indicated that (E+Q)-Lip-Apt has uniform size, good dispersion, and stability.

Table 1 Factor Levels of CoQ10-Lip

Levels	Factors			
	A: Power (W)	B: Time (min)	C: PC: Chol (molar ratio)	D: CoQ10: Lipid (W/W)
1	50	5	2:1	1:3
2	75	10	3:1	1:6.5
3	100	15	4:1	1:10

Table 2 Orthogonal Experimental Design and Results of CoQ10-Lip

	A	B	C	D	EE (%)
1	1	1	1	1	44.50
2	1	2	2	2	63.80
3	1	3	3	3	80.64
4	2	1	2	3	82.17
5	2	2	3	1	45.17
6	2	3	1	2	83.10
7	3	1	3	2	66.70
8	3	2	1	3	87.00
9	3	3	2	1	61.82
k_1	62.980	64.457	71.533	50.496	
k_2	70.146	65.322	69.263	71.200	
k_3	71.840	75.187	64.169	83.270	
R_k	8.860	10.73	7.364	32.774	
Main Factor	D > B > A > C				
Recommended	$A_3B_3C_1D_3$				

In Vitro Antioxidant Activity of (E+Q)-Lip-Apt

Results in Figure S1 showed that rhodamine B-labeled liposomes could be taken up by MIN6 cells. Then the CCK-8 results showed that (E+Q)-Lip-Apt had no significant effect on the cell viability in the concentration range of 0.057–1.71 μM, and the cell viability remained above 90% (Figure 3A). Then, to investigate whether (E+Q)-Lip-Apt could enhance cell viability under oxidative stress, we induced an in vitro oxidative stress model by treating MIN6 cells with 200 μM TBHP for 24 h. The CCK-8 results showed that the cell viability was significantly reduced in the TBHP group and could not be improved in the Ext-4 group, but significantly improved in the (E+Q)-Lip-Apt group ($P < 0.01$ or $P < 0.001$, Figure 3B), indicating that (E+Q)-Lip-Apt could increase the cell survival rate in the range of 0.057~1.71 μM in oxidative stress. Importantly, the (E+Q)-Lip-Apt exhibited the best protective effect in the concentration of 0.285 μM (Figure 3B), so this concentration was used to explore further the in vitro anti-oxidative stress effect of (E+Q)-Lip-Apt. Under oxidative stress conditions, intracellular MDA levels are elevated. Compared with the control group, the MDA levels in the TBHP group were significantly elevated and significantly decreased in the Ext-4 group and (E+Q)-Lip-Apt group ($P < 0.001$, Figure 3C). Importantly, the MDA levels in the (E+Q)-Lip-Apt group were significantly lower than those in the Ext-4 group ($P < 0.05$, Figure 3C), suggesting that (E+Q)-Lip-Apt was more effective in reducing

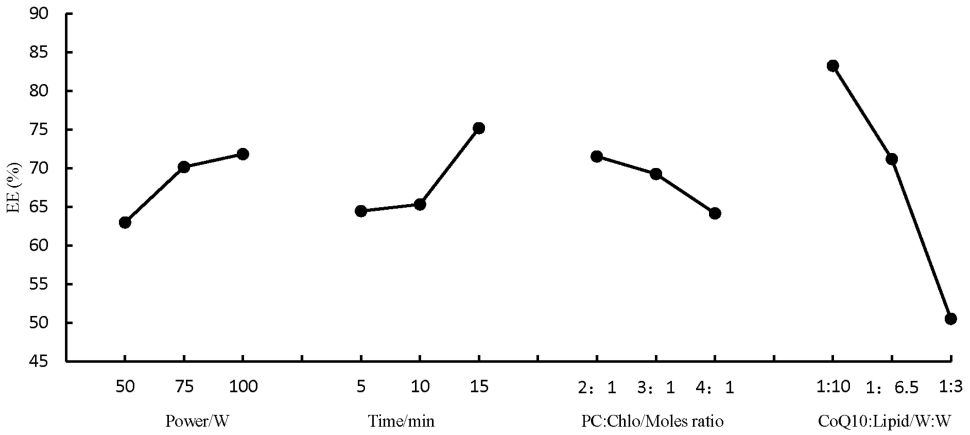

Figure 1 Trend chart of factor levels in CoQ10-Lip.

https://doi.org/10.2147/IJN.S510240

Table 3 Characterization of (E+Q)-Lip-Apt (n=3) ($\bar{x} \pm s$)

	Size(nm)	Zeta potential (mV)	PDI	EE% (Ext-4)	EE% (CoQ10)	CE% (Apt)
CoQ10-Lip	92.7±1.2	−16.6±3.9	0.148±0.148	—	—	—
(E+Q)-Lip	107.4±3.5	−15.2±3.0	0.209±0.034	—	—	—
(E+Q)-Lip-Apt-1 d	112.4±2.2	−16.3±1.9	0.210±0.055	71.59±15.86	98.16±0.20	84.18±6.14
(E+Q)-Lip-Apt-7 d	124.1±2.5	−13.4±1.3	0.159±0.064	—	—	—
(E+Q)-Lip-Apt-18 d	137.3±3.0	−14.8±1.4	0.269±0.137	—	—	—

Abbreviations: Apt, aptamers; Ext-4, exenatide-4; CoQ10, coenzyme Q10; (Q+E)-Lip-Apt, aptamer-functionalized co-loading Ext-4 and CoQ10 liposomes; EE, encapsulation efficiency; CE, aptamer conjugation efficiency; PC, phosphatidylcholine; Chol, cholesterol; PC: Chol, the molar ratio of PC to Chol; CoQ10: lipids, the mass ratio of CoQ10 to lipids.

intracellular lipid oxidation levels when cells undergo oxidative stress. Furthermore, to investigate whether (E+Q)-Lip-Apt achieved its protective effect by scavenging intracellular ROS, DCFH-DA probe was applied to assess the intracellular ROS levels. As shown in (Figure 3D), following 200 μM TBHP treatment for 6 h, the green fluorescence enhancement in the TBHP group, while exposure of MIN6 cells to Ext-4 in the presence of TBHP could not decrease the enhanced green fluorescence. A significant reduction in the green fluorescence signal was noted in the (E+Q)-Lip-Apt group, indicating that intracellular ROS was cleared by (E+Q)-Lip-Apt, and the ROS level was significantly decreased. These results suggested that (E+Q)-Lip-Apt may improve oxidative stress and restore cell viability by scavenging ROS.

High glucose levels would increase ROS levels and oxidative damage to mitochondria. The mitochondrial membrane potential is one of the functional indicators of mitochondria.[25] Thus, the mitochondrial function of MIN6 cells was further investigated. As shown in (Figure 3E), JC-1 existed in the mitochondrial matrix as a polymeric form in normal cells, and obvious red fluorescence could be observed. After treatment with 200 μM TBHP for 24 h, the red fluorescence

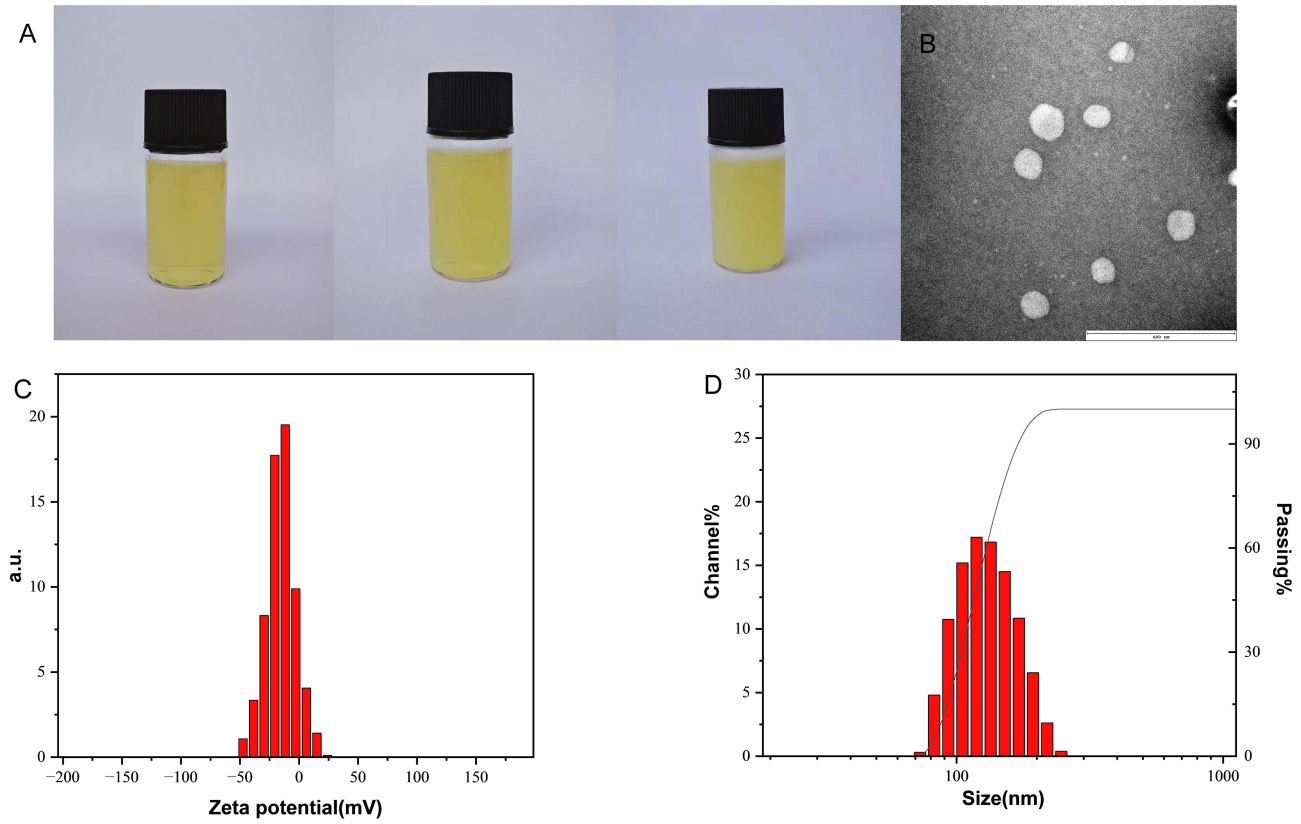

Figure 2 Characterization of (E+Q)-Lip-Apt (**A**) Appearance on day 1, 7, and 18 of preparation; (**B**) TEM morphology, scale bar: 400 nm; (**C**) Size distribution on the first day; (**D**) ZP distribution on the first day.

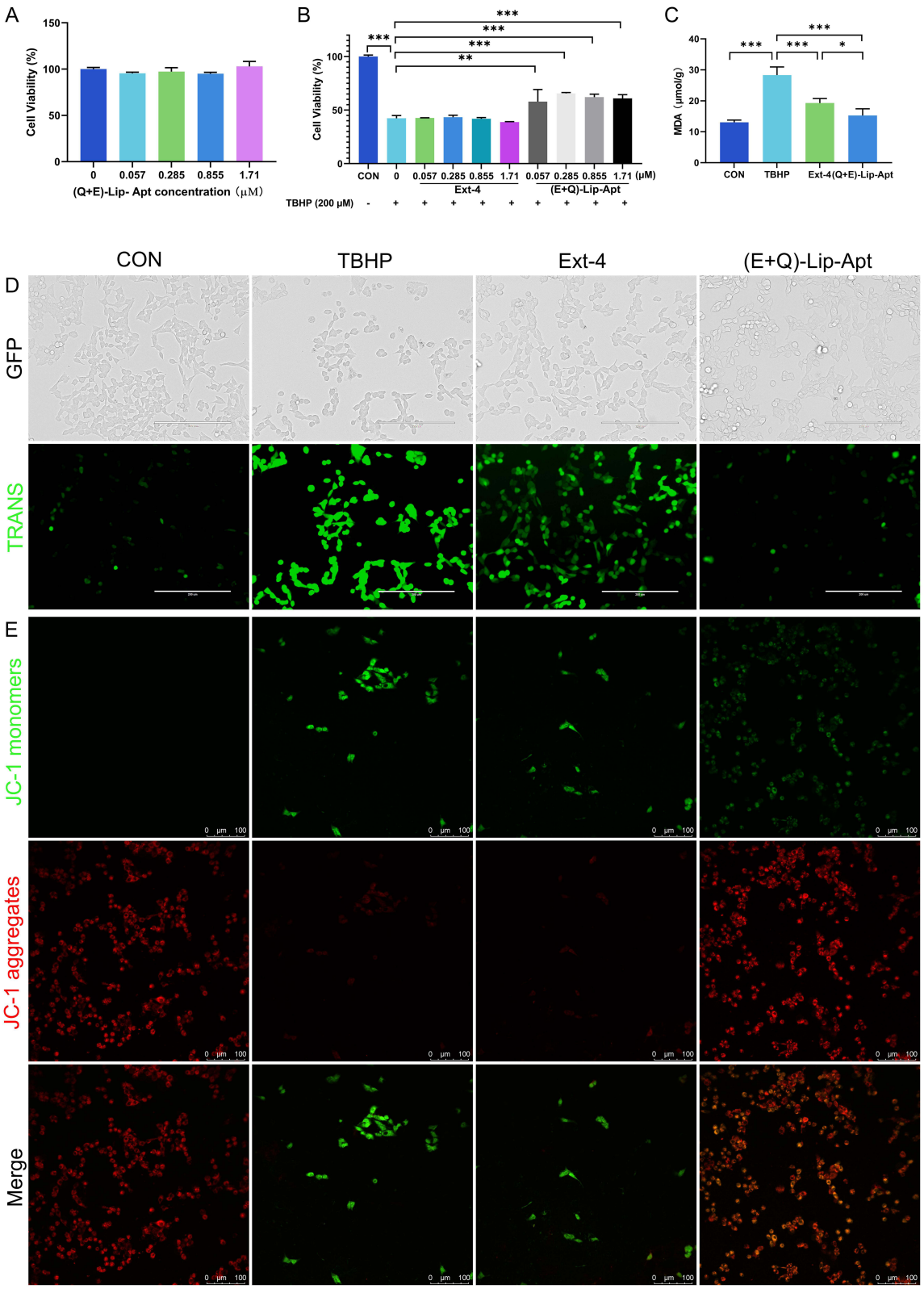

Figure 3 In vitro antioxidant activity of (E+Q)-Lip-Apt. (**A**) Biocompatibility Analysis of (E+Q)-Lip-Apt; (**B**) Cell viability; (**C**) MDA levels; (**D**) DCFH-DA, scale bar: 200 μm; (**E**) JC-1, scale bar: 100 μm. The data were expressed as $\bar{x} \pm s$, n=3. *$P < 0.05$, **$P < 0.01$, ***$P < 0.001$.

https://doi.org/10.2147/IJN.S510240

of cells in the TBHP group significantly decreased, while the green fluorescence significantly increased, which indicated that the mitochondrial membrane potential significantly decreased and mitochondrial dysfunction. The Ext-4 treatment group could not improve the decreased mitochondrial membrane potential. While, distinct green fluorescence could not be detected in the (E+Q)-Lip-Apt group, suggesting recovery of mitochondrial function.

In Vivo Targeting Analysis of (E+Q)-Lip-Apt

To assess the pancreatic targeting ability of (E+Q)-Lip-Apt, the internal organs of mice undergoing (E+Q)-Lip-Apt treatment were imaged using Small Animal In Vivo Imaging System. Figure 4 showed the organs' representative fluorescence images and the quantitative comparison results of average fluorescence intensity. These results indicated that (E+Q)-Lip-Apt was primarily concentrated in the pancreas, suggesting that (E+Q)-Lip-Apt had a high affinity for the pancreas and exhibited good pancreatic targeting ability.

Anti-T2DM Effects of (E+Q)-Lip-Apt

FBG was first conducted to assess the effect of (E+Q)-Lip-Apt in T2DM mice. As shown in (Figure 5A), the FBG of T2DM mice was significantly higher, and decreased significantly under the treatment of Ext-4 and (E+Q)-Lip-Apt. Subsequently, the effect of (E+Q)-Lip-Apt on the improvement of glucose tolerance in T2DM mice was further analyzed by OGTT. The results in (Figure 5B) showed that the blood glucose of mice in the CON group slightly increased and then

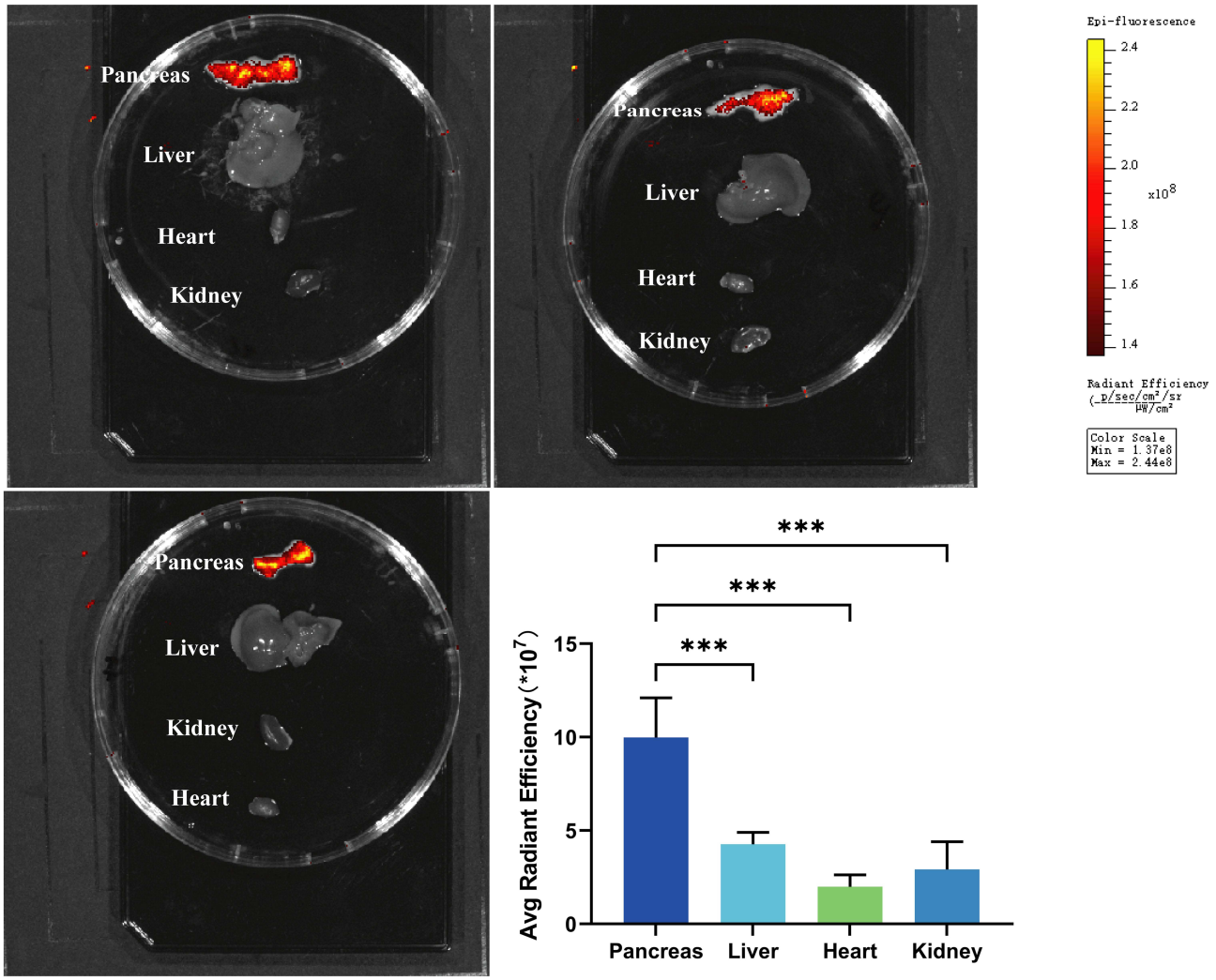

Figure 4 Representative fluorescence images of organs and quantitative results of mean fluorescence intensity. Data were expressed as $\bar{x} \pm s$, n=3. ***$P < 0.001$.

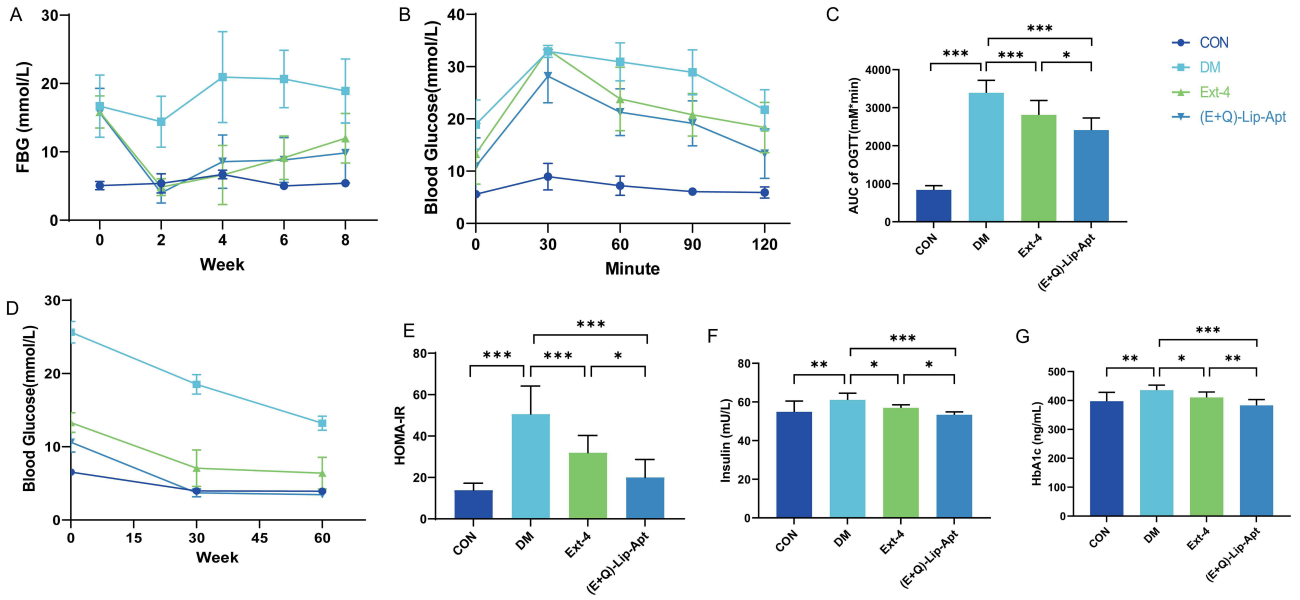

Figure 5 In vivo anti-diabetic effects of (E+Q)-Lip-Apt. (**A**) FBG; (**B and C**) OGTT and AUC of OGTT; (**D**) IPITT; (**E**) HOMA-IR; (**F**) Insulin; (**G**) HbA1c. The data were expressed as $\bar{x} \pm s$. *$P < 0.05$, **$P < 0.01$, ***$P < 0.001$.

recovered to the normal value, which indicated that the mice exhibited a normal glucose tolerance capacity. The blood glucose levels of mice in the T2DM group were significantly higher than those in other groups at all time points, suggesting seriously impaired glucose tolerance in T2DM mice. Compared with the Ext-4 group, the blood glucose values of the (E+Q)-Lip-Apt group were lower, and these results were consistent with the AUC results of the OGTT in (Figure 5C), which indicated that both Ext-4 and (E+Q)-Lip-Apt improved glucose tolerance in T2DM mice, but the improvement effect of (E+Q)-Lip-Apt was more obvious.

Subsequently, the therapeutic effect of (E+Q)-Lip-Apt on insulin resistance was also analyzed by IPITT. The results showed that mice in the control group were sensitive to insulin, and their blood glucose decreased significantly after insulin injection. The blood glucose in the DM group was higher than the normal value at 60 min after insulin injection, which indicated that insulin resistance had occurred. Treatment with Ext-4 and (E+Q)-Lip-Apt could obviously improve insulin resistance of T2DM mice, with their blood glucose progressively declining and approaching the normal value (Figure 5D). Results in (Figure 5E) showed that in comparison with the control group, HOMA-IR levels were significantly elevated in T2DM mice ($P < 0.001$). Treatment with Ext-4 or (E+Q)-Lip-Apt significantly decreased the HOMA-IR level ($P < 0.001$), and it was noteworthy that the HOMA-IR in the (E+Q)-Lip-Apt group was significantly lower than that in the Ext-4 group ($P < 0.05$).

Studies have shown that serum insulin levels in T2DM mice often appear elevated due to the development of insulin resistance and compensatory secretion of insulin.[6] As shown in (Figure 5F), the serum insulin levels were significantly increased in T2DM mice ($P < 0.01$) but significantly decreased to near normal levels after treatment with Ext-4 or (E+Q)-Lip-Apt ($P < 0.05$ or $P < 0.001$). Besides, compared to the Ext-4 group, the serum insulin levels in the (E+Q)-Lip-Apt group were lower ($P < 0.05$), indicating that (E+Q)-Lip-Apt had a more significant effect on improving insulin resistance and compensatory insulin secretion.

The detection of glycosylated hemoglobin (HbA1c) represents a simplistic yet dependable approach to the diagnosis of diabetes, and it has already been employed clinically as a diagnostic guideline. As shown in (Figure 5G), HbA1c levels were significantly increased in T2DM mice ($P < 0.01$) and reduced after treatment with Ext-4 or (E+Q)-Lip-Apt ($P < 0.05$ or $P < 0.001$). Notably, (E+Q)-Lip-Apt was more effective than Ext-4 in reducing HbA1c levels ($P < 0.01$). All these data demonstrated that compared to Ext-4, (E+Q)-Lip-Apt possessed a better therapeutic effect in the treatment of T2DM mice.

https://doi.org/10.2147/IJN.S510240

Improvement Effect of (E+Q)-Lip-Apt on the Structure and Function of the Liver and Pancreas

The liver is one of the target organs of insulin, and the regulation of blood glucose by the liver depends on the blood insulin level and the sensitivity to insulin. Insulin resistance is closely related to abnormalities in liver lipid metabolism.[6] The levels of TG, TC, and LDL-C were significantly elevated in the DM group ($P < 0.001$), indicating lipid metabolism abnormalities in T2DM mice and lipid accumulation in the liver. After treatment with Ext-4 and (E+Q)-Lip-Apt, the levels of TG, TC, and LDL-C in diabetic mice were significantly reduced ($P < 0.001$). It was worth noting that, regardless of the ability to clear TG, TC, or LDL-C from the liver, (E+Q)-Lip-Apt significantly outperformed Ext-4 ($P < 0.05$ or $P < 0.001$) (Figure 6A–C). To investigate whether the effect of lipid clearance was related to the improvement of (E+Q)-Lip-Apt on hepatic oxidative stress, liver MDA content and SOD activity were further measured. The results showed that the liver MDA levels in T2DM mice were significantly higher than those in normal mice ($P < 0.05$). Ext-4 could not improve the elevated liver MDA, but (E+Q)-Lip-Apt could significantly reduce liver MDA levels ($P < 0.01$) (Figure 6D). SOD is an important antioxidant enzyme. Compared to normal mice, the SOD activity in T2DM mice was impaired ($P < 0.01$). Although Ext-4 treatment could improve FBG and insulin resistance in T2DM, it could not restore the impaired SOD activity. Notably, in addition to enhancing the FBG and insulin resistance, (E+Q)-Lip-Apt could also significantly increase the SOD activity in the liver of T2DN mice ($P < 0.01$) (Figure 6E). The above results indicated that (E+Q)-Lip-Apt may enhance the liver's lipid metabolism capacity by improving hepatic oxidative stress.

Subsequently, the pathological changes in the mouse liver were assessed via Hematoxylin-eosin (H&E) staining (Figure 6F). In normal mice, liver cells were arranged in a single-row structure centered around the central vein. In the DM group, liver cells were disordered, with significant infiltration of inflammatory cells, the appearance of round vacuoles of varying sizes and high tension within the cells, the cell nucleus pushed to one side, and obvious fatty degeneration. In the Ext-4 group and (E+Q)-Lip-Apt group, the inflammatory cell infiltration and the intercellular vacuoles were reduced, and the arrangement tended to be neat. The improvement effect of (E+Q)-Lip-Apt was more noticeable.

Thereafter, the pancreatic H&E and insulin Immunohistochemistry (IHC) staining were carried out to assess pancreatic function. The results (Figure 6G) showed that the pancreatic islets of normal mice were spherical cell clusters, the β-cells in the islets were tightly arranged, the inter-cellular capillaries were abundant, and the IHC staining area was relatively large and the color was clear (Figure 6H). However, in T2DM mice, the number of pancreatic islets was reduced, the size became smaller, the arrangement of pancreatic islet β-cells was unclear, and the cells were necrotic. Meanwhile, the IHC staining area of pancreatic islets in T2DM mice was smaller and the color became unclear distinctly. Ext-4 and (E+Q)-Lip-Apt could improve these lesions, and the islets of the T2DM mice treated with (E+Q)-Lip-Apt were normalized, the number and the size of islets increased significantly. Moreover, the IHC results demonstrated that (E+Q)-Lip-Apt exhibited a superior improvement in the pancreatic islet, with the area and quantity of insulin-positive β cells increasing significantly. All these data demonstrated that (E+Q)-Lip-Apt manifested a superior therapeutic efficacy in restoring the liver and pancreas damages induced by oxidative stress and maintaining the functions of liver and pancreatic β-cells in T2DM mice.

Discussion

As early as 1982, oxidative stress had been discovered in laboratory diabetes.[3] Oxidative stress refers to the excessive production and/or reduced clearance of reactive molecules such as ROS and reactive nitrogen species (RNS), which disturbs the balance between ROS production and antioxidant defense function in the body.[26] In a high-glucose state, β-cells are particularly susceptible to attack by ROS, and their regenerative potential is extremely limited.[8] Oxidative stress-mediated pathophysiological mechanisms such as autoimmune reaction, inflammation, insulin resistance, hyperglycemia/glucotoxicity, and lipotoxicity, typically occur in diabetic conditions. These pathophysiological processes will lead to various types of β cell death, such as apoptosis, necrosis, necroptosis, ferroptosis, and autophagy,[4] which is extremely detrimental to diabetic patients. Moreover, oxidative stress can also lead to reduced antioxidant enzyme activity,[27] mitochondrial dysfunction,[28] reduced insulin secretion, and insulin resistance.[6] Besides, many researches have indicated that oxidative stress is also involved in the mechanisms of various diabetic complications, such as diabetic retinopathy,[28] endothelial dysfunction,[29] diabetic nephropathy,[30] and so on. Existing antidiabetic drugs mainly exert their

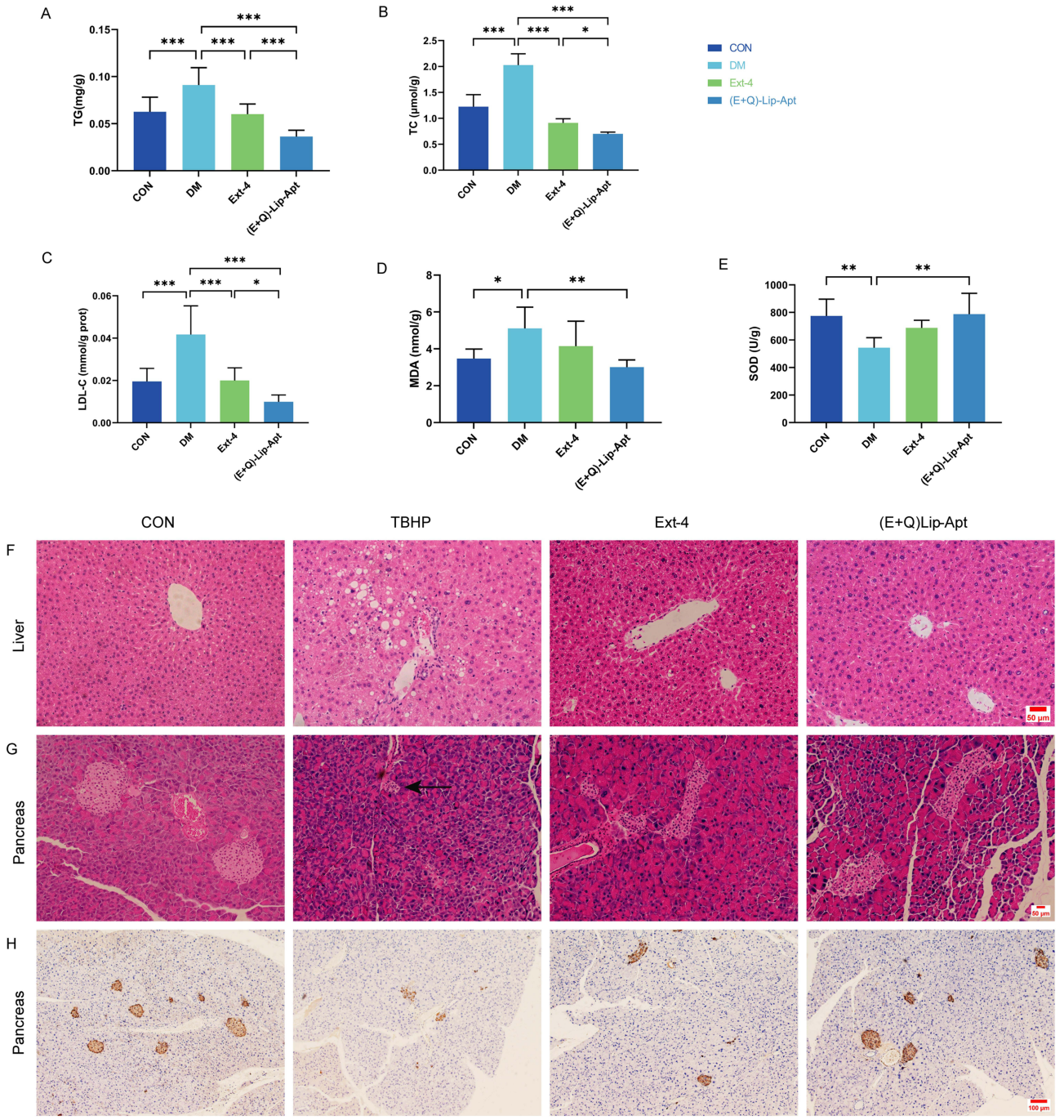

Figure 6 The improvement effect of (E+Q)-Lip-Apt on the structure and function of the liver and pancreas. (**A**) TG; (**B**) TC; (**C**) LDL-C; (**D**) MDA; (**E**) SOD. (**F and G**) H&E staining of the liver and pancreas, scale bar: 50 μm; (**H**) Insulin IHC staining, scale bar: 100 μm. The data were expressed as $\bar{x} \pm s$. *$P < 0.05$, **$P < 0.01$, ***$P < 0.001$.

effects by promoting insulin secretion, reducing hepatic gluconeogenesis, increasing peripheral glucose uptake, or delaying intestinal glucose absorption. However, it does not fundamentally solve the problem, as a significant number of diabetic patients still cannot control their blood glucose levels and endure many adverse reactions, such as weight gain, allergic reactions and even life-threatening hypoglycemia.[4,6,31] Most importantly, the aforesaid therapy cannot restore the dysfunction of β-cells and maintain their amount.[4,6] Therefore, improving oxidative stress and thereby ensuring the survival and function of pancreatic β-cells may be key to the treatment of diabetes and its complications.

https://doi.org/10.2147/IJN.S510240

Dietary antioxidants were commonly used in clinical practice, such as CoQ10.[3] However, they exhibited restricted therapeutic efficacy owing to their inferior water solubility, poor stability, poor gastrointestinal absorption, and subeffective concentration in the target tissue.[3,4,32] Therefore, our study established a novel antioxidant system based on liposomes to achieve targeted antioxidation and ensure the efficacy of antioxidants. The optimal composition and physical characterization of (E+Q)-Lip-Apt were investigated in this study. The results showed that (E+Q)-Lip-Apt was successfully constructed with high loading efficacy, uniform size and shape, and a diameter of approximately 110 nm.

Our results showed that TBHP-induced oxidative stress resulted in reduced survival, diminished antioxidant capacity, and decreased mitochondrial membrane potential in MIN6 cells. We assumed that (E+Q)-Lip-Apt improved damaged β-cells through antioxidant effects. The results indicated that Ext-4 could not scavenge intracellular ROS and also failed to enhance the viability of MIN6 cells. However, after treatment with (E+Q)-Lip-Apt, MIN6 cells exhibited decreased levels of intracellular ROS and MDA, increased mitochondrial membrane potential, and enhanced cell viability more effectively. It indicated that oxidative stress impaired β-cells, leading to β-cell death, and (E+Q)-Lip-Apt protected MIN6 cells through their antioxidant effects.

Targeted drug delivery can elevate the drug concentration in the requisite area, and thereby enhance the therapeutic efficacy. The (E+Q)-Lip-Apt we constructed with active target capacity to the pancreas via binding to the aptamers of pancreatic polypeptide. The in vitro imaging results showed that compared to other organs, the pancreas exhibited significant fluorescence, indicating that (E+Q)-Lip-Apt displayed a strong affinity for the pancreas and could achieve active targeting antioxidation. Moreover, it indicated that the aptamers of pancreatic polypeptide could achieve an ideal targeting capability in the treatment of T2DM for antioxidation.

The therapeutic effects of (E+Q)-Lip-Apt on the functionality and mass of β cells were also validated in vivo. The T2DM mice we constructed exhibited typical diabetic symptoms during the experiment, with elevated FBG levels, significantly reduced glucose tolerance, and decreased insulin sensitivity,[33,34] along with elevated liver MDA levels, reduced SOD activity, and obvious liver lesions. It indicated that oxidative stress has occurred in diabetic mice. The application of (E+Q)-Lip-Apt was capable of reversing these alterations in T2DM mice. Additionally, it was worth noting that the H&E and IHC results showed significant pathological changes occurring in the diabetic pancreas, with damage to the structure and function of the islet β-cells. Similarly, we assumed that (E+Q)-Lip-Apt could improve damaged β-cells through antioxidant effects in vivo. It could be seen that, although Ext-4 had good anti-diabetic effects, it could not improve the function of damaged pancreatic β-cells. In contrast, (E+Q)-Lip-Apt not only exhibited more pronounced anti-glycemic effects but also reduced MDA levels and enhanced SOD activity. Compared to Ext-4, (E+Q)-Lip-Apt could more prominently improve the pancreatic lesions, specifically manifested by an increase in the number and area of islets, a shape closer to a spherical form, and clearer, bigger staining areas in IHC, indicating the structure and function of pancreatic β-cells have been restored. These results confirmed that oxidative stress was closely related to the structure and function of pancreatic β-cells. In the report of Deng et al, the protective effects of antioxidants on β-cells have also been confirmed.[8] (E+Q)-Lip-Apt facilitated the accumulation of Ext-4 and CoQ10 in the pancreas, achieving anti-glycemic and antioxidant effects, reducing oxidative stress, and restoring the function of pancreatic β-cells. Hence, the strategy of antioxidant stress exhibited great potential in the treatment of β-cell death and diabetes.

Conclusion

In summary, a dual-drug-loaded liposome with pancreatic targeting capacity was successfully constructed. (E+Q)-Lip-Apt possessed excellent characteristics as a nano drug carrier, with good dispersion and stability, and high drug encapsulation efficiency. The antioxidant activity effects bestowed by CoQ10 endued (E+Q)-Lip-Apt with a superior protective effect on the structure and function of pancreatic β-cells. Therefore, targeted antioxidant strategies are expected to become a new direction for diabetes treatment.

Abbreviations

Apt, aptamers; Ext-4, exenatide-4; CoQ10, coenzyme Q10; (Q+E)-Lip-Apt, aptamer-functionalized co-loading Ext-4 and CoQ10 liposomes; EE, encapsulation efficiency; CE, aptamer conjugation efficiency; PC, phosphatidylcholine; Chol, cholesterol; PC: Chol, the molar ratio of PC to Chol; CoQ10: lipids, the mass ratio of CoQ10 to lipids; TBHP, Tert-Butyl Hydroperoxide; ROS, reactive oxygen species; FBG, fasting blood glucose.

Ethics Approval and Informed Consent

All animal experiments were conducted with the approval of the Animal Ethics Committee of Guangdong Medical University [Approval No.: GDY2102488].

Acknowledgments

This work is supported via funding from "The expression mechanism and regulatory strategies of eccDNA in paclitaxel resistance in breast cancer(2KZ21049)."

Author Contributions

All authors made a significant contribution to the work reported, whether that is in the conception, study design, execution, acquisition of data, analysis and interpretation, or in all these areas; took part in drafting, revising or critically reviewing the article; gave final approval of the version to be published; have agreed on the journal to which the article has been submitted; and agree to be accountable for all aspects of the work.

Funding

This work was supported by Youth Fund of the National Natural Science Foundation of China (number 82204435). GuangDong Basic and Applied Basic Research Foundation (number 2021B1515140060).

Disclosure

The authors report no conflicts of interest in this work.

References

1. Sun H, Saeedi P, Karuranga S, et al. IDF diabetes atlas: global, regional and country-level diabetes prevalence estimates for 2021 and projections for 2045. *Diabet Res Clin Pract*. 2022;183:109119. doi:10.1016/j.diabres.2021.109119
2. Zheng Y, Ley SH, Hu FB. Global aetiology and epidemiology of type 2 diabetes mellitus and its complications. *Nat Rev Endocrinol*. 2018;14(2):88–98. doi:10.1038/nrendo.2017.151
3. Zhang P, Li T, Wu X, Nice EC, Huang C, Zhang Y. Oxidative stress and diabetes: antioxidative strategies. *Front Med*. 2020;14(5):583–600. doi:10.1007/s11684-019-0729-1
4. Dinić S, Arambašić Jovanović J, Uskoković A, et al. Oxidative stress-mediated beta cell death and dysfunction as a target for diabetes management. *Front Endocrinol*. 2022;13:1006376. doi:10.3389/fendo.2022.1006376
5. Schatz DA, Winter WE. Autoimmune markers in diabetes. *Clin Chem*. 2011;57(2):168–175. doi:10.1373/clinchem.2010.148205
6. Li X, Zhen M, Zhou C, et al. Gadofullerene nanoparticles reverse dysfunctions of pancreas and improve hepatic insulin resistance for type 2 diabetes mellitus treatment. *ACS Nano*. 2019;13(8):8597–8608. doi:10.1021/acsnano.9b02050
7. Nauck MA, Quast DR, Wefers J, Meier JJ. GLP-1 receptor agonists in the treatment of type 2 diabetes – state-of-the-art. *mol Metab*. 2021;46(4):101102. doi:10.1016/j.molmet.2020.101102
8. Deng W, Wang H, Wu B, Zhang X. Selenium-layered nanoparticles serving for oral delivery of phytomedicines with hypoglycemic activity to synergistically potentiate the antidiabetic effect. *Acta Pharmaceutica Sinica B*. 2019;9(1):74–86. doi:10.1016/j.apsb.2018.09.009
9. Hargreaves I, Heaton RA, Mantle D. Disorders of human coenzyme Q10 metabolism: an overview. *Int J mol Sci*. 2020;21(18):6695. doi:10.3390/ijms21186695
10. Maheshwari RA, Parmar GR, Hinsu D, Seth AK, Balaraman R. Novel therapeutic intervention of coenzyme Q10 and its combination with pioglitazone on the mRNA expression level of adipocytokines in diabetic rats. *Life Sci*. 2020;258(22):118155. doi:10.1016/j.lfs.2020.118155
11. Szabová J, Mišík O, Havlíková M, Lízal F, Mravec F. Influence of liposomes composition on their stability during the nebulization process by vibrating mesh nebulizer. *Colloids Surf B Biointerfaces*. 2021;204(8):111793. doi:10.1016/j.colsurfb.2021.111793
12. Hammoud Z, Gharib R, Fourmentin S, Elaissari A, Greige-Gerges H. New findings on the incorporation of essential oil components into liposomes composed of lipoid S100 and cholesterol. *Int J Pharm*. 2019;561(8):161–170. doi:10.1016/j.ijpharm.2019.02.022
13. Dymek M, Sikora E. Liposomes as biocompatible and smart delivery systems – the current state. *Adv Colloid Interface Sci*. 2022;309(11):102757. doi:10.1016/j.cis.2022.102757
14. Zhu M, Zhu S, Liu Q, Ren Y, Ma Z, Zhang X. Selenized liposomes with ameliorative stability that achieve sustained release of emodin but fail in bioavailability. *Chin Chem Lett*. 2023;34(1):107482. doi:10.1016/j.cclet.2022.04.080
15. Xie Q, Deng W, Yuan X, et al. Selenium-functionalized liposomes for systemic delivery of doxorubicin with enhanced pharmacokinetics and anticancer effect. *Eur J Pharm Biopharm*. 2018;122:87–95. doi:10.1016/j.ejpb.2017.10.010
16. Oliveira R, Pinho E, Sousa AL, DeStefano JJ, Azevedo NF, Almeida C. Improving aptamer performance with nucleic acid mimics: de novo and post-SELEX approaches. *Trends Biotechnol*. 2022;40(5):549–563. doi:10.1016/j.tibtech.2021.09.011
17. Ni S, Zhuo Z, Pan Y, et al. Recent progress in aptamer discoveries and modifications for therapeutic applications. *ACS Appl Mater Interfaces*. 2021;13(8):9500–9519. doi:10.1021/acsami.0c05750
18. Zhang Y, He J, Shen L, et al. Brain-targeted delivery of obidoxime, using aptamer-modified liposomes, for detoxification of organophosphorus compounds. *J Control Release*. 2021;329(1):1117–1128. doi:10.1016/j.jconrel.2020.10.039

19. Guan B, Zhang X. Aptamers as versatile ligands for biomedical and pharmaceutical applications. *Int J Nanomed*. 2020;15:1059–1071. doi:10.2147/IJN.S237544
20. McConnell EM, Holahan MR, DeRosa MC. Aptamers as promising molecular recognition elements for diagnostics and therapeutics in the central nervous system. *Nucleic Acid Ther*. 2014;24(6):388–404. doi:10.1089/nat.2014.0492
21. Monaco I, Camorani S, Colecchia D, et al. Aptamer functionalization of nanosystems for glioblastoma targeting through the blood–brain barrier. *J Med Chem*. 2017;60(10):4510–4516. doi:10.1021/acs.jmedchem.7b00527
22. Wong K-Y, Liu Y, Zhou L, Wong M-S, Liu J. Mucin-targeting-aptamer functionalized liposomes for delivery of cyclosporin A for dry eye diseases. *J Mater Chem B*. 2023;11(21):4684–4694. doi:10.1039/d3tb00598d
23. Śliwińska-Mossoń M, Milnerowicz H. Distribution of pancreatic polypeptide–secreting endocrine cells in nondiabetic and diabetic cases. *Appl Immunohistochem Mol Morphol*. 2017;25(6):422–431. doi:10.1097/PAI.0000000000000310
24. Qin S, Chen N, Yang X, et al. Development of dual-aptamers for constructing sandwich-type pancreatic polypeptide assay. *ACS Sens*. 2017;2(2):308–315. doi:10.1021/acssensors.6b00836
25. Cao Y, Chen Z, Hu J, et al. Mfn2 regulates high glucose-induced MAMs dysfunction and apoptosis in podocytes via PERK pathway. *Front Cell Dev Biol*. 2021;9(1):769213. doi:10.3389/fcell.2021.769213
26. Niu F, Liu W, Ren Y, et al. β-cell neogenesis: a rising star to rescue diabetes mellitus. *J Adv Res*. 2024;62:71–89. doi:10.1016/j.jare.2023.10.008
27. Lu M-C, Zhao J, Liu Y-T, et al. CPUY192018, a potent inhibitor of the Keap1-Nrf2 protein-protein interaction, alleviates renal inflammation in mice by restricting oxidative stress and NF-κB activation. *Redox Biol*. 2019;26(7):101266. doi:10.1016/j.redox.2019.101266
28. Kang Q, Yang C. Oxidative stress and diabetic retinopathy: molecular mechanisms, pathogenetic role and therapeutic implications. *Redox Biol*. 2020;37(10):101799. doi:10.1016/j.redox.2020.101799
29. An Y, B-t X, S-r W, et al. The role of oxidative stress in diabetes mellitus-induced vascular endothelial dysfunction. *Cardiovasc Diabetol*. 2023;22(1):237. doi:10.1186/s12933-023-01965-7
30. Ricciardi CA, Gnudi L. Kidney disease in diabetes: from mechanisms to clinical presentation and treatment strategies. *Metabolism*. 2021;124(11):154890. doi:10.1016/j.metabol.2021.154890
31. Zhang X, Qi J, Lu Y, He W, Li X, Wu W. Biotinylated liposomes as potential carriers for the oral delivery of insulin. *Nanomedicine*. 2014;10(1):167–176. doi:10.1016/j.nano.2013.07.011
32. Mahjoob M, Stochaj U. Curcumin nanoformulations to combat aging-related diseases. *Ageing Res Rev*. 2021;69(5):101364. doi:10.1016/j.arr.2021.101364
33. Li X, Zhu J, Wang T, et al. Antidiabetic activity of Armillaria mellea polysaccharides: joint ultrasonic and enzyme assisted extraction. *Ultrason Sonochem*. 2023;95(4):106370. doi:10.1016/j.ultsonch.2023.106370
34. Lee Y-S, Lee D, Park G-S, et al. Lactobacillus plantarum HAC01 ameliorates type 2 diabetes in high-fat diet and streptozotocin-induced diabetic mice in association with modulating the gut microbiota. *Food Funct*. 2021;12(14):6363–6373. doi:10.1039/d1fo00698c